ChemPubSoc Europe

DOI: 10.1002/cctc.201901910

CHEMCATCHEM Full Papers

Benchtop NMR for Online Reaction Monitoring of the Biocatalytic Synthesis of Aromatic Amino Alcohols

C. Claaßen,[a] K. Mack,[a, b] and D. Rother*[a, b]

Online analytics provides insights into the progress of an ongoing reaction without the need for extensive sampling and offline analysis. In this study, we investigated benchtop NMR as an online reaction monitoring tool for complex enzyme cascade reactions. Online NMR was used to monitor a two-step cascade beginning with an aromatic aldehyde and leading to an aromatic amino alcohol as the final product, applying two different enzymes and a variety of co-substrates and intermediates. Benchtop NMR enabled the concentration of the reaction components to be detected in buffered systems in the single-digit mM range without using deuterated solvent. The concentrations determined via NMR were correlated with offline samples analyzed via uHPLC and displayed a good correlation between the two methods. In summary, benchtop NMR proved to be a sensitive, selective and reliable method for online reaction monitoring in (multi-step) biosynthesis. In future, online analytic systems such as the benchtop NMR devices described might not only enable direct monitoring of the reaction, but may also form the basis for self-regulation in biocatalytic reactions.

Introduction

Enzymatic reactions typically show high substrate specificities and both regio- and stereoselectivities, making them ideal alternatives to classical chemical synthesis strategies. This especially holds true if products with one or more chiral centers and high optical purity are desired.[1] Ongoing research in the field of biocatalysis provides a broad variety of well-characterized enzymes catalyzing reactions that are extremely challenging with classical chemical synthesis.[2] The variety of enzymes available provides access to a steadily increasing number of different products.[3]

Within the field of biocatalysis, the combination of enzymes into multi-step reaction cascades has been increasingly investigated over the past decade.[4] The product range accessible in enzymatic cascade reactions increases with each additional reaction step.[5] However, not only the accessible product range increases, but also the overall complexity of the reaction design. Among other aspects, major challenges in designing suitable enzyme cascades include side reactions due to enzyme-substrate promiscuity,[4h,6] and balancing the different reaction steps to achieve optimal conversions and specific space-time yields for the whole cascade. Detailed kinetic knowledge about the reactions would help, for example, in selecting the right time point at which a cascade step reaches its peak, so that the next reaction step could be started when using a sequential cascade mode (i.e. by adding the enzyme for the next reaction step). Another point is optimal balancing of the amounts of catalyst in modularly attached reactors (i.e. plug-flow devices). Selecting suitable amounts of catalyst would be greatly facilitated if sensitive and selective online analytics were available for each reaction step and the overall process performance. Furthermore, if the performance of complex reactions or multi-step synthesis could be suitably monitored, it would be easier to establish optimal reaction parameters for the whole system in a more time-efficient manner.

Recent advances with benchtop NMR (nuclear magnetic resonance) spectroscopy makes online reaction monitoring possible not only for chemical syntheses,[7] but also for fermentation processes,[8] and biocatalytic reactions[9] where low analyte concentrations and the necessity of using deuterated solvents has impeded the use of NMR in the past. A detailed overview of the advantages and disadvantages of benchtop NMR for online reaction monitoring in general can be found in references.[7d,10] With respect to the monitoring of biocatalytic reactions, online NMR offers advantages such as the possibility of analyzing the reaction mixture without destroying or changing the sample composition and without the need for extensive sampling. Altogether, this prevents the loss of valuable product due to sampling and analysis. In addition to the above-mentioned advantages, NMR in general enables reaction components to be determined which can be extremely challenging to quantify with other analytical techniques, but which frequently serve as reaction components in biocatalytic synthesis, e.g. isopropylamine[4a,h,11] or acetaldehyde.[1a,12] The

[a] Dr. C. Claaßen, K. Mack, Prof. Dr. D. Rother
Institute of Bio- and Geosciences – Biotechnology (IBG-1)
Forschungszentrum Jülich GmbH
52425 Jülich (Germany)
E-mail: do.rother@fz-juelich.de
[b] K. Mack, Prof. Dr. D. Rother
Aachen Biology and Biotechnology (ABBt)
RWTH Aachen University
52074 Aachen (Germany)

Supporting information for this article is available on the WWW under https://doi.org/10.1002/cctc.201901910

This publication is part of a joint Special Collection with ChemBioChem on "Excellence in Biocatalysis Research". Please follow the link for more articles in the collection.

distinct advantages mentioned above, are expected to lead to an increasing relevance of NMR for applications in biotechnological systems as already indicated by the first few publications in this field.[8a,9]

In this contribution, we use the example of an chiral aromatic amino alcohol to show that substrates and products for the enzymatic cascade reaction leading to 3-(2-amino-1-hydroxypropyl) phenol, originally published by Erdmann et al.,[4h] are detectable in a buffered solution even in a low milli-molar range using the benchtop NMR device. We show the signals of various buffers and alternative co-substrates. Since a suitable distinction between the NMR signals of the reaction components is given, concentrations of the different compounds can be calculated even in the complex reaction mixture. In this way, we propose benchtop NMR-based online analysis for the biocatalytic cascade reaction to gain direct insights into product formation during the cascade reaction without the need for extensive sampling. Furthermore, direct information can be gained by means of the proposed online reaction monitoring, thus enabling a quicker reaction to parameter changes or in the future external regulation of the system.

Results and Discussion

The cascade reaction monitored here by NMR-based online analysis is the sequential two-step cascade reaction to (1*S*,2*S*)-3-(2-amino-1-hydroxypropyl)phenol (3OH-AHP) previously published in a similar mode by Erdmann *et al.* for another stereoisomer, the (1*R*,2*S*)-stereoisomer.[4h] The cascade consists of two reaction steps, where first 3-hydroxy-benzaldehyde (3OH-BA) is converted by a carboligase to 1-hydroxy-1-(3-hydroxyphenyl) propan-2-one (3OH-PAC). The second reaction step, a reductive amination, catalyzed by a transaminase with an amine donor molecule as co-substrate, leads to the final amino alcohol (3OH-AHP).

In general, the access to four different stereoisomers of 3OH-AHP is possible by the combination of enzymes with different stereoselectivities.[4h] For this publication, the (1*S*,2*S*)-stereoisomer was chosen for online reaction monitoring. The stereoisomer was obtained by combining the *S*-selective carboligase *Ap*PDC E469G[13] with an *S*-selective transaminase *Bm*TA[14] (see Scheme 1). This cascade is especially interesting as the active catalyst in both steps has to be sensitively regulated to avoid undesired by-product formation or else the steps have to be separated in time or space.[4h] To run the overall cascade efficiently, optimal concentrations of both enzymes and all participating co-substrates are needed, which are usually obtained by extensive process optimization on a small scale. With these prerequisites, the cascade is a good example for online analytics to directly monitor process design and selectivity to the final product.

Cascade design

To assess whether signal overlap in the NMR spectrum will occur between the reaction components during online measurements, firstly offline spectra of each pure component in aqueous solution were measured with the benchtop NMR device. Signal overlaps between the reaction components would complicate data evaluation. However, it should be noted, that signal overlaps do not necessarily prevent the usage of NMR spectroscopy for online analytics. Nevertheless, for this publication we chose the simplest system to verify the general suitability of NMR analytics for enzyme cascades in buffered systems.

Figure 1 shows the positioning of the signals occurring from the substrates/products (A), two possible co-substrates for the first reaction step (B), three possible amine donors/resulting by-products in the second reaction step (C), and five alternative buffers and water (D) in the 60 MHz benchtop NMR applied in this study. The original spectra of the components in water can be found in the supporting information. The aldehyde-CH- and CH_3-signals of the substrates/products were clearly separated in the NMR spectra, making it easy to distinguish between the different components. However, the CH-protons of 3OH-PAC and 3OH-AHP were buried under the broad water signal.

The signal width, especially of the water signal, was strongly dependent on the system shim status (Figure 1-D, top row): As indicated by the darker coloring, the water signal was relatively narrow, even without any water suppression, if the system had a very good shim status (signal width at 50% height: 0.28 Hz; signal width at 0.55% height: 6.3 Hz; for the standard shimming sample, 10% H_2O in D_2O). If the shim status was not optimal (signal width at 50% height: 0.69 Hz; signal width at 0.55% height: 15.63 Hz; for the standard shimming sample, 10% H_2O

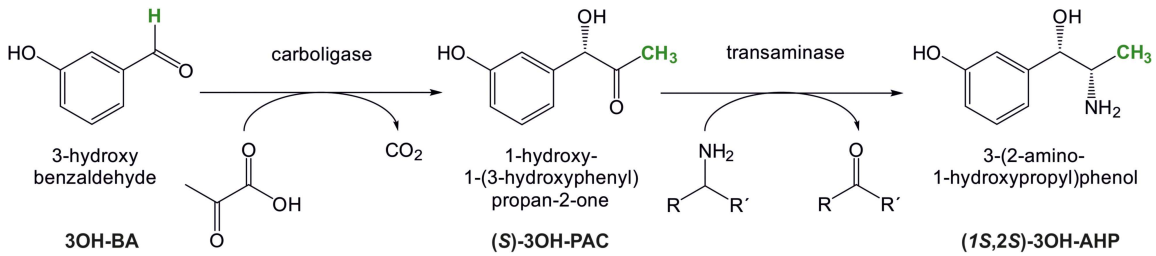

Scheme 1. Reaction scheme of a two-step enzymatic cascade yielding the aromatic amino alcohol 3-(2-amino-1-hydroxypropyl)phenol in (1*S*,2*S*)-conformation. R=CH_3; R'=CH_3, COOH, or phenyl depending on the amine donor applied. The proton groups monitored by NMR-based online analytic in this publication are highlighted in dark green.

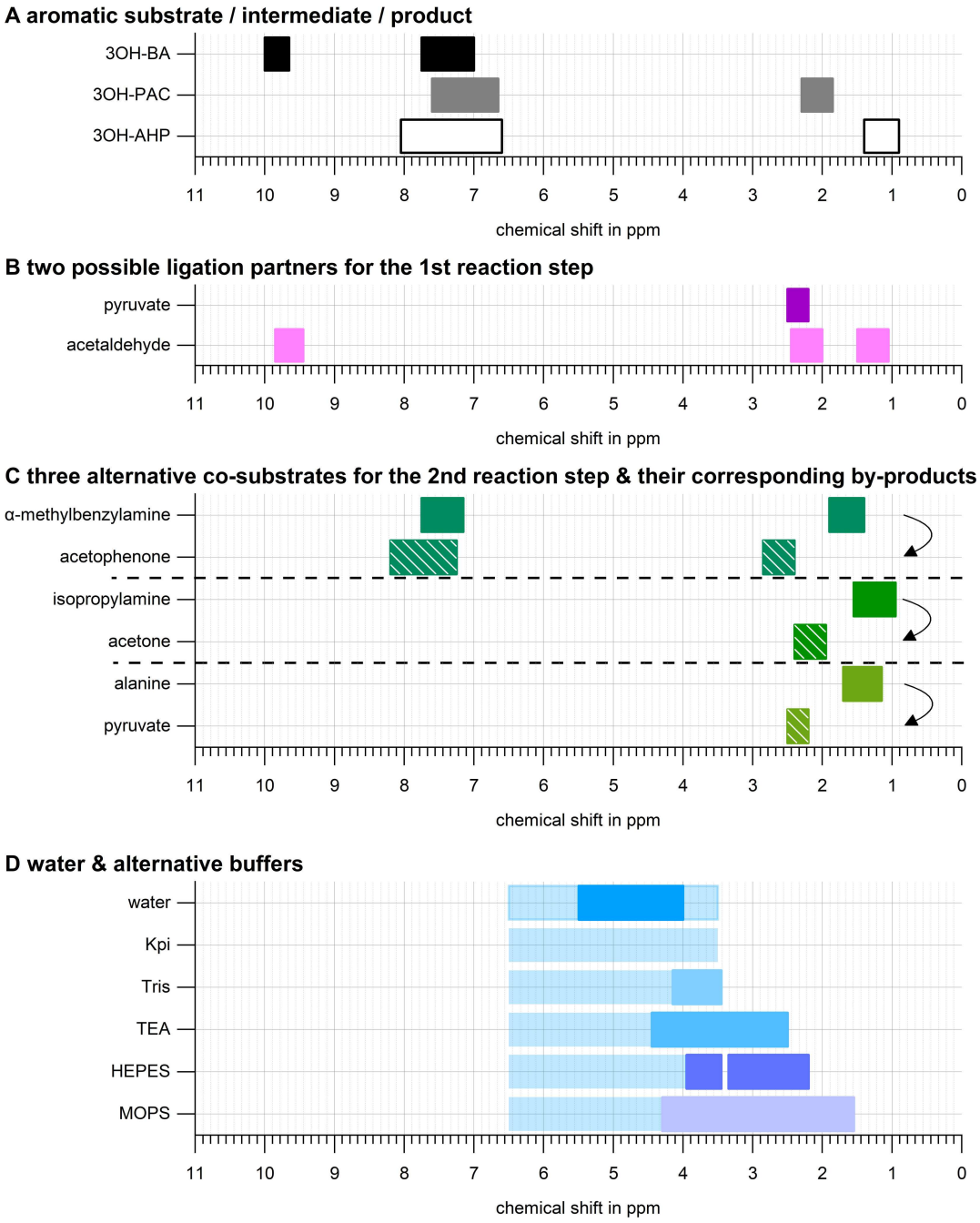

Figure 1. Position of NMR-signals of the reaction components, co-substrates, by-products and buffers for the cascade reaction. Some signals for the substrates/products and buffers, especially CH-protons, were (partly) buried under the water signal so that these signals are not shown in the figure. Corresponding amine donors and their keto-products formed upon amino-group transfer in C are indicated by the arrows. Water signal is also shown in the buffer spectra in D. (3OH-BA = 3-hydroxy-benzaldehyde; 3OH-PAC = 1-hydroxy-1-(3-hydroxyphenyl) propan-2-one; 3OH-AHP = 3-(2-amino-1-hydroxypropyl) phenol).

in D_2O), a broader water signal was observed, as indicated by the light blue coloring.

With respect to the investigated buffer systems, Kpi buffer did not contribute additional signals to the spectra besides the water signal, and the signal of Tris-buffer was almost in the same ppm range as the water signal, while for the other buffers (TEA, HEPES and MOPS) signals in addition to the water signal occurred between 1.55 ppm and the water signal. If a product signal in this ppm range is to be monitored, the use of these buffers is not recommended, as buffers are typically applied at higher concentration than the substrates. This will most likely lead to the substrate signal being completely buried under the buffer ("blind region"). For our purposes, Kpi buffer was chosen as it is a suitable buffer for the two-step cascade to the amino alcohol[4h] and moreover has a lack of additional signals except

for the water signal thus preventing signal overlap with reaction components during reaction monitoring.

The situation becomes more complicated with respect to the carboligation partner for the first reaction step (Figure 1-B) and a number of possible amine donors (Figure 1-C). For the first reaction step, an overlap was found between the aldehyde CH of 3OH-BA (@ 9.82 ppm) and acetaldehyde (AA) (@ 9.65 ppm), as well as an overlap between the CH_3-group of 3OH-PAC (@ 2.07 ppm) and CH_3-group of AA (@ 2.20 ppm), which is to be expected due to the line width in the 60 MHz spectra. The signal of pyruvate (@ 2.33 ppm) was in the same range as the CH_3-group of 3OH-PAC (@ 2.07 ppm). However, sufficient separation of the signals seems to be more likely here. Pyruvate is not only a good reaction partner for 3OH-BA after decarboxylation through the carboligase enzyme, but furthermore the acid derivatives have typically been shown to be less toxic for the enzyme compared to the free aldehyde.[15] Therefore, pyruvate was chosen as the partner for carboligation and for further analysis.

For the second reaction step, possible signal overlaps cannot be precluded for isopropylamine (IPA), alanine, and their ketone by-products with 3OH-PAC and 3OH-AHP. For our purposes, α-MBA and acetophenone were the best monitorable amine donors/acceptors and were not only selected because of this advantage, but also due to the fact that α-MBA pushed the reaction equilibrium to the product side without the need of further adjustments.[16]

The signals used for quantification of substrate, intermediate and product were the aldehyde CH of 3OH-BA (@ 9.82 ppm), the CH_3-group of 3OH-PAC (@ 2.07 ppm) and the CH_3-group of 3OH-AHP (@ 1.08 ppm). Here, a suitable distinction is expected between the reaction components, while the aromatic protons of the components overlap largely in the NMR spectra. Whether or not a signal overlap will ultimately occur, is largely dependent on the concentration of the components and the current operational status, especially line width, of the NMR spectrometer. This parameter closely correlates with the shim status of the system, where a manual correction to obtain optimal operational status proved to be difficult during the experiments.

NMR measuring parameters

The system which was used for online reaction monitoring is depicted in Figure 2. It consists of the Spinsolve60^{ULTRA} 60 MHz NMR spectrometer with a glass measuring capillary, a peristaltic pump and a computer with the control software. The measuring capillary has a widened part serving as the measuring cell, with the diameter of the measuring cell corresponding to the diameter of a standard NMR tube (5 mm; a scheme of the measuring cell with dimensions can be found in the supporting information). The reaction vessel was linked to the peristaltic pump and the measuring capillary with standard HPLC tubing (Ø 3 mm).

Before starting online reaction monitoring, a number of parameters that are important to ensure correct quantification were determined with offline NMR samples. These data are shown in the following subsections. Subsequently, we give the results of the online reaction monitoring for the selected cascade and correlate the data collected from the online NMR measurements with offline samples analyzed via uHPLC.

Relaxation time

To ensure correct quantification of NMR signals, the longitudinal relaxation time (T_1) is one of the most important values.[17] Relaxation describes the process of dynamic return of the spins to the initial equilibrium state after a pulse experiment and T_1 is

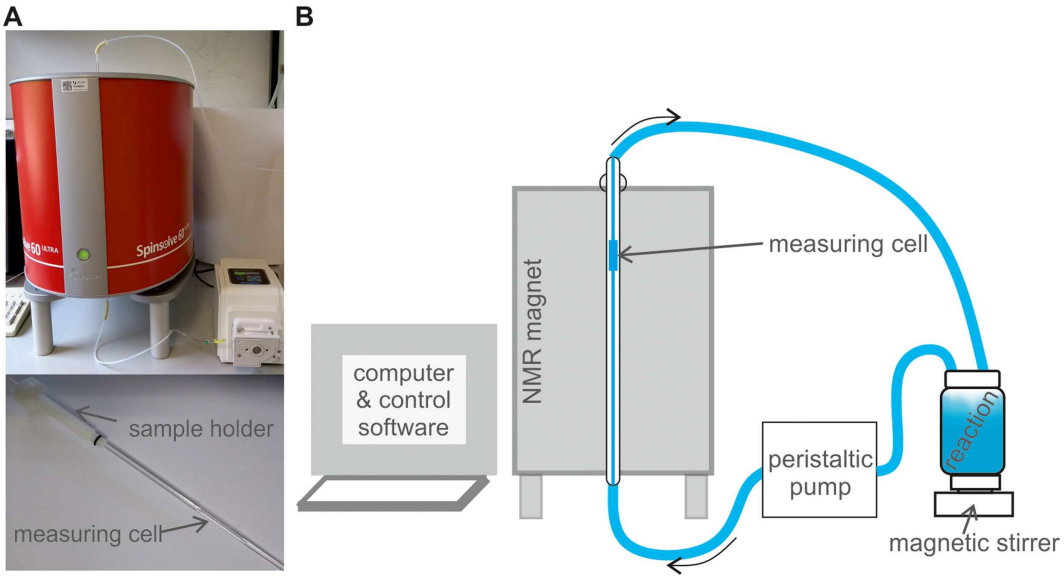

Figure 2. A) NMR setup (top) and measuring capillary adjusted in the sample holder (bottom); B) scheme of the NMR setup.

the time that this process takes.[18] It should be noted that individual T_1-times are not substance constants, but dependent on experimental conditions i.e. solvent, magnetic field strength, temperature etc.

For correct quantification, the time between two pulse experiments (spectrum scans) should be at least 5-[8a,17,19] to 7-times[20] the value of the relaxation time to ensure that all spins (99.9% in the case of $7\times T_1$[20]) have returned to the initial state before starting the next pulse sequence. If the time between the scans is less than 5- to 7-times T_1, the signal intensity will successively decrease and is then no longer directly correlated with the concentration of the component. The highest T_1-time of a signal intended to be used for calculating concentrations therefore determines the waiting time between two scans.

T_1-times were measured with an inversion recovery pulse sequence. For this pulse sequence, a 180° pulse is applied to the sample, switching the magnetization antiparallel to the magnetic field; then spectra are measured with a standard 90° pulse after different evolution times (max. 15 sec in this publication). If the applied time between the two pulses is less than ln(2)*T_1-time, negative integral values are measured. T_1-times were calculated by fitting the curve according to the formula given in the experimental section.

Figure 3 shows the relaxation times of the protons used for quantification in online reaction monitoring. It is obvious that there were major differences between the relaxation time of the 3OH-AHP CH_3-group with 0.71 s, the 3OH-PAC CH_3-group with 2.37 s and the 3OH-BA aldehyde CH-proton with 4.05 s. The differences in the T_1-times were expected from the molecular structure of the components and are in accordance with literature.[21] A detailed discussion of the differences in the relaxation times of the components would go beyond the scope of this publication; interested readers are referred to the publications with reference number[22] for further information. Taking into account the longest T_1-time of the aldehyde CH-proton of 3OH-BA and the required factor 7, the time between acquisitions of spectra has to be at least 28.35 s. For all further experiments, the repetition time between the scans was therefore set to 30 s.

Limit of quantification

The limit of quantification (LOQ) was determined using a concentration series of substrate (3OH-BA), intermediate (3OH-PAC) and final product (3OH-AHP) in the range of 2.5 mM–25 mM, and determining the signal-to-noise ratio (SNR) depending on the number of scans used for spectra acquisition. The LOQ was defined as the concentration value where the SNR was ten, which is an appropriate value according to literature,[17,23] and was calculated from linear regression. It should be noted that the SNR is additionally dependent on the shim status of the spectrometer. A very good shim status results in generally higher SNRs and smaller line widths leading to lower LOQs, while a non-optimal shim status results in lower SNRs and broader signals leading to higher LOQs. The data shown below were acquired with an average shim status for the standard shimming sample (signal width at 50% height: 0.41 Hz; signal width at 0.55% height: 11.6 Hz; 10% H_2O in D_2O). For a very good shim status, even lower LOQs are possible.

As shown in Figure 4, the LOQs decreased with increasing number of scans, due to the reduction of the noise in the spectra resulting from repeated measurement. While LOQs were between 3.7 mM (3OH-PAC) and 9.5 mM (3OH-AHP) for only one scan, repetitions up to 16 spectra led to LOQs between 0.8 mM (3OH-PAC) and 2.8 mM (3OH-AHP). LOQs for 3OH-BA were between these values with 8.4 mM for one scan and 2.7 mM for 16 scans. The difference in LOQs between the investigated components can be explained by the number of protons and multiplicity of the signals. For 3OH-PAC, the signal to be monitored is a CH_3-group without neighboring protons meaning that the signal occurs as a singlet. For 3OH-BA, the signal is a singlet as well, but only has one aldehyde proton. Therefore, the intensity of the signal was lower compared to

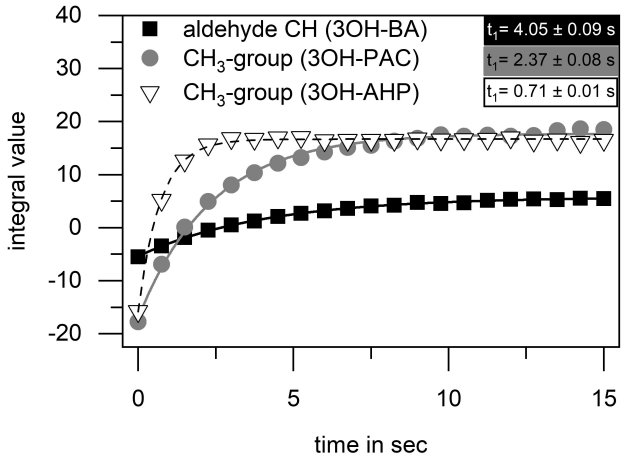

Figure 3. Relaxation times of protons that are intended to be used for calculating concentrations during the reaction. ($n=3$).

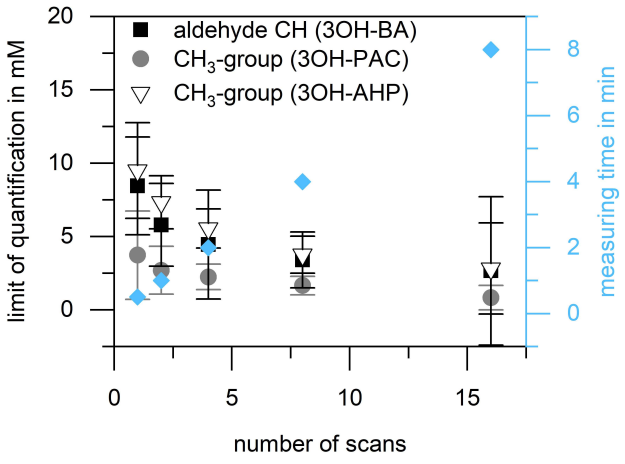

Figure 4. Left axis: Limit of quantification for educt and products of the enzymatic cascade depending on the number of scans. Right axis: Measuring time for one spectrum depending on the number of scans. ($n=3$).

the 3OH-PAC at the same concentration. For 3OH-AHP, the signal to be followed is a CH_3-group just like for 3OH-PAC, but this time the CH_3-group has a neighboring proton, meaning that the signal occurs as a duplet, again with lower intensity compared to the singlet, which has three protons in 3OH-PAC.

The data clearly shows that low detection limits can be reached with the benchtop NMR, but always at the expense of measuring time and therefore time resolution. This means that the optimal measuring parameters are always a tradeoff between measuring time and detection limit. For very slow reactions, 8 min of measuring time might be applicable, while for very fast reactions even 2 min of measuring time might be too long for the collection of appropriate kinetic data. For this publication, 4 scans corresponding to a measuring time of 2 min and resulting quantification limits of 4.5 mM for 3OH-BA, 2.2 mM for 3OH-PAC and 5.5 mM for 3OH-AHP (all at average shim status) were chosen for online reaction monitoring.

Influence of pumping speed on signal intensity

Earlier studies showed that above a certain pumping speed the premagnetization of the sample in the NMR magnet is no longer sufficient thus leading to a decrease in signal intensity and an increase in line width.[7a] As this decrease in signal intensity leads to the signal no longer being directly correlated with the concentration, pumping speeds slower than those leading to decreases in signal intensity have to be chosen for online reaction monitoring. If it is not possible to stick to rather low pumping speeds e.g. due to experimental limitations, correction factors accounting for the specific intensity decrease can be used as an alternative.[24]

Figure 5 depicts the percentage change of the signal intensity at different pumping speeds based on the signal intensity without pumping for the signals to be quantified during reaction monitoring. A decrease in signal intensity of the aldehyde CH-proton of 3OH-BA was determined for pumping speeds higher than 10 rpm (corresponding to 1.5 mL min^{-1}) while for the CH_3-groups of 3OH-PAC and 3OH-AHP no pronounced signal decreases were noted up to 20 rpm (corresponding to 3 mL min^{-1}). That spins with higher relaxation time are more prone to signal decrease with increasing pumping speed is well known from literature.[24] Consequently, to preclude any effects of signal decrease on 3OH-BA due to pumping, a pumping speed lower than 1.5 mL per minute, i.e. 3.5 rpm corresponding to 0.51 mL min^{-1}, was chosen for online reaction monitoring in continuous flow.

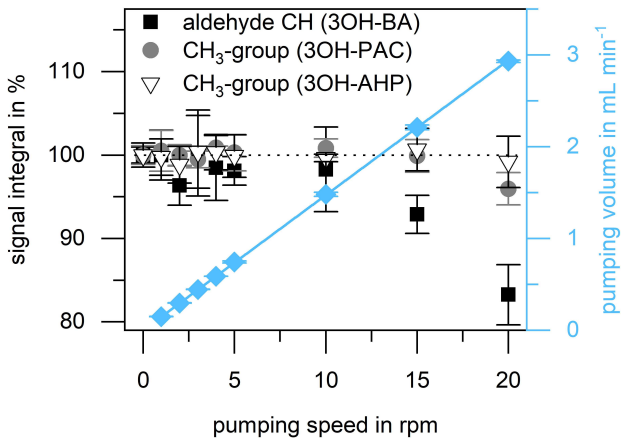

Figure 5. Left axis: Signal integral depending on the pumping speed in % of the integral without pumping. (100 % = signal integral without pumping) Right axis: Pumping volume per minute depending on the pumping speed. ($n = 3$).

Online reaction monitoring

For online reaction monitoring, 3-(trimethylsilyl)-2,2,3,3-tetradeuteropropionic acid (TMSP-d_4) was added to the reaction mixture to serve as an internal standard for calculating the concentrations. TMSP-d_4 was chosen as internal standard, as it has a good water solubility, showed no visible signal overlap with the compounds to be followed via reaction monitoring, and additionally showed no interference with the enzymes and the overall cascade reaction. The detected T_1-time was with 2.85 s sufficiently low to allow correct quantification (compare previous chapter). Data obtained from online NMR measurements were correlated with data obtained from samples taken during the reaction analyzed with uHPLC.

Figure 6 shows the data obtained during reaction monitoring of the carboligation reaction. Depending on the reaction time (Figure 6-A; time increases from bottom to top), the NMR spectra show rapid changes: The aldehyde proton of 3OH-BA at 9.82 ppm was already invisible in the fourth spectrum (corresponding to a reaction time of 28 min), while the signal of 3OH-PAC increased successively with the decrease of the 3OH-BA. Other changes in the spectra were visible in the aromatic protons region (6.5 ppm–7.7 ppm), but since an overlap between the signals of 3OH-BA and 3OH-PAC was evident there, a more detailed evaluation was not undertaken. Additionally, the appearance of the CH-proton of 3OH-PAC at 5.27 ppm, partly superimposed with the water signal, was detected.

To have a closer look at the reaction, concentrations (Figure 6-B) were calculated based on the integrals of the CH-aldehyde proton of 3OH-BA, the CH_3-group of 3OH-PAC and the CH_3-group of pyruvate (T_1-value of 4.53 s). The NMR-based initial concentration for 3OH-BA was corrected by the emerging amount of 3OH-PAC since the reaction was very fast and the first measurement was taken after approx. 3 min as the solution first had to be pumped into the measuring capillary. The corrected initial concentration of 57.2 mM 3OH-BA showed good correlation with the applied concentration of 3OH-BA (60 mM), while the initial concentration value determined for pyruvate (124 mM ± 5 mM) was lower than the expected amount (140 mM). One factor explaining this deviation could have been the T_1-time of the CH_3-group of pyruvate, which would require a repetition time of 31.92 s to be fully quantitative. This deviation can however only account for an approximately 0.55 % (= 0.77 mM) lower detected concentration of pyruvate compared to the expected concentration and was

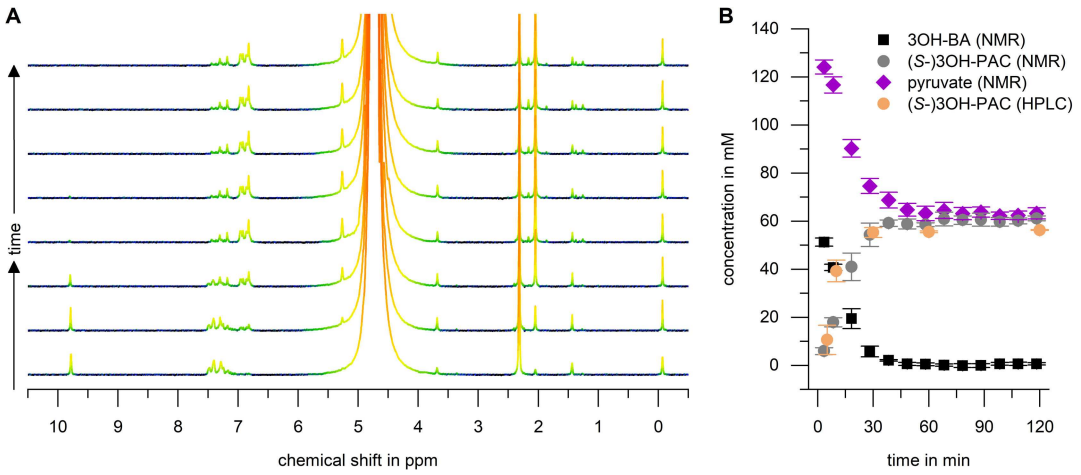

Figure 6. Online reaction monitoring for the carboligation reaction. A: Examples of NMR spectra recorded during the reaction; from bottom to top measurements were taken after 3.4 min, 8.4 min, 18.3 min, 28.2 min, 38.3 min, 48.4 min, 58.3 min, and 68.4 min; B: Concentrations for reaction compounds determined by NMR measurement and product additionally by uHPLC analysis (orange dots). Data were obtained with very good shim status of the system. (HPLC $n=2$; NMR $n=3$).

therefore ruled out as main factor. The reason for the deviation between detected and expected pyruvate concentration is most likely a combination of the purity of pyruvate (an additional signal occurs already in the pure substance, see supporting information), and its relatively fast degradation in water.

For the first part of the cascade, the carboligation reaction, it can be seen, that all the concentrations depicted in Figure 6-B reached a plateau corresponding to complete conversion of the aldehyde after approx. 40 min of reaction time. In total, a final concentration of 60.4 mM ± 1.6 mM was measured for the intermediate 3OH-PAC via NMR. With uHPLC a final concentration of 56.3 mM ± 0.2 mM for 3OH-PAC was determined, which was slightly lower compared to the NMR data, but nevertheless indicated the same reaction progression. In summary, the deviation between the concentration values of the two methods was 7%, which is a good correlation, especially as uHPLC and NMR are two completely different analytical methods, which were moreover calibrated differently. uHPLC measurements furthermore confirmed complete conversion of the 3OH-BA.

Figure 7 shows the data obtained for reaction monitoring of the second part of the cascade, the reductive amination. The NMR- spectra shown over time in Figure 7-A (time increasing from bottom to top) indicate gradual changes in the spectra: The CH_3-group signal of 3OH-PAC at 2.05 ppm decreased until it was almost completely disappeared in the last spectrum (corresponding to a reaction time of 24 h). In the same manner the CH_3-groups signal of 3OH-AHP (1.08 ppm) increased. In addition, a decrease in the amine donor signal at 1.60 ppm was visible, as the amino group was transferred to the final product

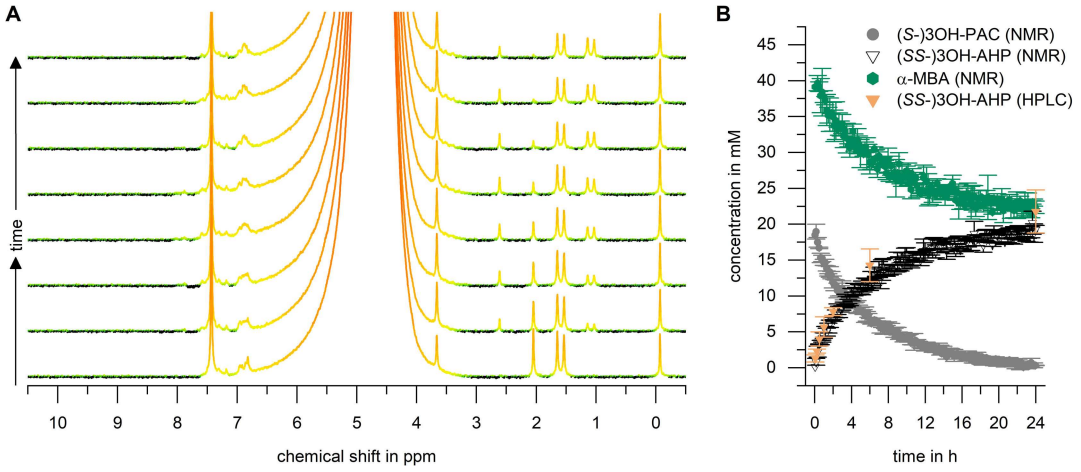

Figure 7. Online reaction monitoring for the reductive amination reaction. A: Examples of NMR spectra recorded during the reaction; from bottom to top measurements were taken after 3.4 min, 2 h, 4 h, 6 h, 10 h, 14 h, 20 h, 24 h; B: Concentrations for reaction compounds determined by NMR measurement and product additionally by uHPLC analysis (orange triangles). Data were obtained with average shim status of the system. ($n=3$).

and the amine donor formed acetophenone (CH_3-groups signal at 2.61 ppm).

The concentrations (Figure 7-B) were calculated based on the integrals of the CH_3-groups of 3OH-PAC, 3OH-AHP and α-MBA (T_1-value of 1.11 s). Again, the initially measured concentrations (after 3 min of reaction time due to filling of the measuring capillary) of 18.5 mM for 3OH-PAC and 39.1 mM for α-MBA showed a good correlation with the amounts applied for 3OH-PAC (20 mM) and α-MBA (40 mM). The concentration of 3OH-PAC decreased successively while the concentration of the final product 3OH-AHP increased, yielding a final concentration of 19.4 mM ± 1.2 mM 3OH-AHP corresponding to a conversion of 97.1% ± 6.2%. For 3OH-PAC, a residual amount of 0.4 mM ± 0.2 mM corresponding to 1.9% ± 1.0% was estimated, while for α-MBA a residual amount of 22.8 mM ± 0.4 mM corresponding to 57% of the applied amount was determined, showing that the mass balances were closed for all three components. The concentrations of 3OH-AHP determined via uHPLC showed the same trend compared to the NMR measurements, but the concentrations determined via uHPLC tended to be higher compared to the values measured with NMR. The measured final concentration via uHPLC was 21.8 mM ± 3.0 mM, and thus 12% higher compared to the NMR measurements.

During the reaction, approx. half of the amount of α-MBA was consumed, corresponding to an equimolar ratio to the product. Interestingly, pretrials also showed that when less than 40 mM of α-MBA was applied, still only approx. half of the amount of α-MBA was converted, indicating that the *Bm*TA most likely can only convert one of the α-MBA enantiomers, as the racemic mixture was applied for the reaction. The kinetic resolution between the two α-MBA enantiomers has been previously described in the literature for a number of different amine-transaminases.[25]

Compared to data for the reductive amination of 3OH-PAC with *Bm*TA and the much smaller isopropylamine as amine donor from our lab (data not shown), reductive amination with α-MBA progressed more slowly. Most likely, a steric effect slows down the reaction when the much more bulky amine donor α-MBA is arranged in the active site together with the substrate. Comparing carboligation reaction and reductive amination, the amination proceeded much more slowly as a quantitative conversion of 60 mM substrate was already achieved in the carboligation after approx. 40 min of reaction time, while reductive amination of 20 mM of substrate took almost 24 h. It is additionally intriguing, that double the mass of purified transaminase was applied for the reaction compared to the carboligase. These data are in general agreement with data previously published for similar cascade reactions[4f–h] so that the online reaction monitoring data confirm these findings. Furthermore, NMR and uHPLC analysis showed identical trends with respect to reaction progression and almost similar reaction times leading to full conversion. In summary, benchtop NMR is very suitable for detecting substrates/intermediates/by-product sensitively and for obtaining direct information on their concentrations while running the reaction.

Conclusions

In this contribution, we showed that substrates and products for the enzymatic cascade reaction leading to the aromatic amino alcohol 3-(2-amino-1-hydroxypropyl)phenol (3OH-AHP) are detectable in a low milli-molar range (approx. 2 mM–5 mM with 2 min measuring time) in buffered aqueous solution using online benchtop NMR. Measurements were performed in standard buffer solution, without the need to apply deuterated solvent or components. Since a suitable distinction between the NMR signals of the reaction components was given, the concentrations of substrates/intermediates/products were calculated directly from the NMR spectra with the help of an internal standard. In the authors' view, the distinction between the NMR signals is one of the most crucial points permitting an easy reaction monitoring, as data evaluation might be much more challenging (or even impossible) for reactions where different signals overlap to a large extent, e.g. due to similar chemical shifts or broader line widths.

For the two-step enzymatic reaction leading to 3OH-AHP online reaction monitoring provided direct information on the concentration of the reaction components during the reaction without the need to take samples. The reaction monitoring was shown to be very sensitive with regard to concentration changes and at the same time very reproducible. Additionally, a high correlation between concentrations determined via online NMR and offline uHPLC samples was shown for the reaction products.

In future, online analytic systems such as the benchtop-NMR device described may also be used for purposes other than direct monitoring of the reaction in (multi-step) biosynthesis. Exemplarily, this technique is believed to be a basis for self-regulation, as it is not only sensitive and selective, but also sufficiently fast. This could be especially helpful for reactions where high product concentrations are so far hard to achieve due to substrate insolubility or substrate toxicity.[26] In these cases, feeding strategies could be set up for implementing feedback-control. Also other types of interaction, such as subsequent catalyst addition, would be adjustable. Furthermore, NMR could enable the quantification of substrates that are extremely hard to analyze with other techniques, e.g. acetaldehyde, to enable better process control for these reactions. Altogether, the possibility of directly controlling the reactions means that optimal regulation, for example, regarding specific space-time yields, may be possible in the near future.

Experimental Section

Materials

3-Hydroxy-benzaldehyde (3OH-BA), alpha-methylbenzylamine (α-MBA), isopropylamine (IPA), acetaldehyde (AA), pyridoxalphosphate (PLP), triethanolamine (TEA), and hydrochloric acid (HCl) were purchased from Sigma-Aldrich (Germany). Acetone, pyruvate, potassium dihydrogenphosphate (KH_2PO_4), di-potassium hydrogenphosphate (K_2HPO_4), 2-[4-(2-hydroxyethyl)piperazin-1-yl]ethanesulfonic acid (HEPES), 3-morpholinopropane-1-sulfonic acid (MOPS),

sodium hydroxide (NaOH), 3-(trimethylsilyl)propionic-2,2,3,3-d4 acid sodium salt (TMSP), trifluoroacetic acid (TFA), diethanolamine (DEA) were purchased from Carl Roth (Germany). Other reagents were purchased from the following sources (given in parentheses): 3-(2-amino-1-hydroxypropyl)phenol (3OH-AHP; TRC, Canada); acetophenone (AlfaAesar, Germany); alanine (Fluka, Germany); thiamine pyrophosphate (ThDP; AppliChem, Germany); 2-amino-2-(hydroxymethyl)propane-1,3-diol (Tris; AlfaAesar, Germany); magnesium chloride hexahydrate ($MgCl_2$*$6H_2O$; Fluka, Germany).

A Magritek Spinsolve 60 MHz NMR spectrometer was used as the NMR system. NMR data were recorded using the Spinsolve 1.15.0 Software and analyzed using Mestrenova (Version 12.4.0-22023). The NMR system was equipped with a LongerPump® BT100-2J (DG-2). As the uHPLC system an Agilent 1290 Infinity II was employed (consisting of solvent rack, temperature-controlled sample rack, temperature-controlled multisampler, temperature-controlled column oven, binary high-speed pump, diode array detector) as well as a ZORBAX RRHD Eclipse Plus C18, 2.1×100 mm, 1.8 μm particle size and a precolumn. Details of sample preparation for uHPLC measurement and uHPLC method can be found in the supporting information. The uHPLC data were recorded and analyzed using Agilent ChemStation software.

Offline NMR measurements

Recording of NMR spectra

NMR spectra of the components were recorded with the 60 MHz Spinsolve NMR spectrometer at concentrations of 25 mM in the case of reaction components as reference and 100 mM in the case of buffers in water. Spectra were recorded with 16 scans per spectrum, an acquisition time of 3.2 s, repetition time of 30 s (time between the pulse experiments) and a pulse angle of 90°.

Determination of relaxation time

Relaxation times were determined for the reaction components at a concentration of 25 mM in water with 4 scans, an acquisition time of 6.4 s, repetition time of 30 s, pulse angle of 90°, max. inversion time of 15 s and 21 steps. The signal integral was fitted to y = B + F*exp(-x*G) with G^{-1} being the relaxation time according to the Mestrenova software package.

Determination of limit of quantification

The limit of quantification (LOQ) was determined by recording spectra of the reaction components in water with different concentrations (2.5 mM, 5 mM, 7.5 mM, 10 mM and 25 mM), and determining the signal-to-noise ratio (SNR) in the spectra for the signal to be quantified. Measuring parameters were an acquisition time of 3.2 s, repetition time of 30 s, pulse angle of 90° and different numbers of scan (1, 2, 4, 8 and 16). Linear regressions of the signal-to-noise ratio for the different numbers of scans were calculated based on SNR and concentration of the sample. With the linear regression, the concentration at a signal-to-noise ratio of 10 was determined (according to the commonly accepted ICH Harmonized Tripartite Guidance Q2(R1)[23]).

Investigation of influence of pumping speed on signal intensity

To investigate the influence of pumping speed on signal intensity, solutions of the reaction compounds with a concentration of 25 mM each were pumped through the measuring capillary at different speeds with a peristaltic pump. NMR spectra were recorded after at least 5 min of continuous pumping (without stopping the pump during NMR signal detection) with 4 scans, an acquisition time of 3.2 s, a repetition time of 30 s and a pulse angle of 90°. The pumping volume per minute resulting from the rotating speed of the peristaltic pump was determined gravimetrically.

Online reaction monitoring

Reaction conditions of the enzymatic transformation

Carboligation: The carboligation reaction was performed with purified enzyme (*Ap*PDC E469G) at a protein concentration of 1.25 mg/mL in 100 mM Kpi buffer at pH 6.5 supplemented with 2.5 mM $MgCl_2$, 0.1 mM ThDP, 0.2 mM PLP and 5 mM TMSP. Substrate concentrations were 60 mM 3OH-BA and 140 mM pyruvate. Reactions were carried out for 2 h at 30 °C.

Reductive amination: Reductive amination was performed with purified enzyme (*Bm*TA) at a protein concentration of 2.5 mg/mL in 100 mM Kpi buffer at pH 7.5 supplemented with 2.5 mM $MgCl_2$, 0.1 mM ThDP, 0.2 mM PLP and 5 mM TMSP. 20 mM of the substrate (*S*)-3OH-PAC was applied and 40 mM of the co-substrate α-MBA was added. Reactions were carried out at 30 °C and allowed to proceed for 24 h.

Reaction monitoring

The enzymatic reaction was set up according to the previous subchapter in a glass reaction vessel with a volume of 50 mL and connected to the tubing of the NMR spectrometer and peristaltic pump. The reaction vessel was sealed with sealing film to prevent evaporation. Directly after adding the enzyme, the program for reaction monitoring was started, beginning by pumping the reaction mixture into the measuring capillary. Due to the dead volume of the tubing and the pumping speed, the first measurement was started after 2.4 min of reaction, when the tubing and capillary were sufficiently filled (i.e. supply line and measuring capillary completely filled; approx. 7 mL). Subsequent measurements were taken every 10 min after running a quick shim protocol to keep the system in optimal configuration during the whole reaction monitoring process. The complete script used for online reaction monitoring with the Spinsolve Software can be found in the supporting information.

Samples for uHPLC analysis were taken after 5 min, 15 min, 30 min, 1 h and 2 h in the case of the carboligation reaction and after 5 min, 15 min, 30 min, 1 h, 2 h, 6 h and 24 h in the case of the reductive amination.

Statistical Analysis

All data are presented as a mean ± standard deviation. Unless stated otherwise, three independent replications of all experiments were performed in this study.

Acknowledgements

The authors are grateful to Prof. Dr. Wolfgang Kroutil (TU Graz) for providing the plasmid for Bm*TA production. The authors would like to thank Cinderella Kempe (FZ Jülich, IBG-1) and Lilia Arnold (FZ Jülich, IBG-1) for assistance with protein expression and purification. The authors received funding from the European*

Research Council (ERC) under the European Union's Horizon 2020 research and innovation program (grant agreement no. 757320) as part of the LightCas (light-controlled synthetic enzyme cascades) project. Further funding was received in frame of the BioSC FocusLab "HyImPAct" (Hybrid processes for Important Precursor and Active pharmaceutical ingredients) by the federal state of North-Rhine Westphalia.

Conflict of Interest

The authors declare no conflict of interest.

Keywords: online analytics · enzyme cascade · benchtop NMR · chiral amino alcohols

[1] a) M. Beigi, E. Gauchenova, L. Walter, S. Waltzer, F. Bonina, T. Stillger, D. Rother, M. Pohl, M. Müller, *Chem. Eur. J.* **2016**, *22*, 13999–14005; b) N. J. Turner, L. Humphreys, *Biocatalysis in organic synthesis: The retrosynthesis approach* **2018**; c) M. Ghaffari-Moghaddam, H. Eslahi, Y. A. Aydin, D. Saloglu, *J. Biol. Methods* **2015**, *2*, e25.

[2] a) H. C. Hailes, D. Rother, M. Müller, R. Westphal, J. M. Ward, J. Pleiss, C. Vogel, M. Pohl, *FEBS J.* **2013**, *280*, 6374–6394; b) I. V. Pavlidis, M. S. Weiß, M. Genz, P. Spurr, S. P. Hanlon, B. Wirz, H. Iding, U. T. Bornscheuer, *Nat. Chem.* **2016**, *8*, 1076; c) R. Westphal, C. Vogel, C. Schmitz, J. Pleiss, M. Müller, M. Pohl, D. Rother, *Angew. Chem. Int. Ed.* **2014**, *53*, 9376–9379; d) S. E. Payer, J. H. Schrittwieser, B. Grischek, R. C. Simon, W. Kroutil, *Adv. Synth. Catal.* **2016**, *358*, 444–451; e) W. Zhang, E. Fernández-Fueyo, Y. Ni, M. van Schie, J. Gacs, R. Renirie, R. Wever, F. G. Mutti, D. Rother, M. Alcalde, F. Hollmann, *Nat. Can.* **2018**, *1*, 55–62.

[3] a) A. S. Bommarius, B. R. Riebel-Bommarius, *Biocatalysis: Fundamentals and applications*, Wiley-VCH, Weinheim, **2004**; b) K. Faber, *Biotransformations in organic chemistry: A textbook, 6th ed.*, Springer-Verlag, Heidelberg, **2011**; c) M. T. Reetz, *J. Am. Chem. Soc.* **2013**, *135*, 12480–12496.

[4] a) P. Both, H. Busch, P. P. Kelly, F. G. Mutti, N. J. Turner, S. L. Flitsch, *Angew. Chem. Int. Ed.* **2016**, *55*, 1511–1513; b) A. Jakoblinnert, D. Rother, *Green Chem.* **2014**, *16*, 3472–3482; c) I. Oroz-Guinea, E. García-Junceda, *Curr. Opin. Chem. Biol.* **2013**, *17*, 236–249; d) E. Ricca, B. Brucher, J. H. Schrittwieser, *Adv. Synth. Catal.* **2011**, *353*, 2239–2262; e) P. A. Santacoloma, G. Sin, K. V. Gernaey, J. M. Woodley, *Org. Process Res. Dev.* **2011**, *15*, 203–212; f) T. Sehl, H. C. Hailes, J. M. Ward, R. Wardenga, E. von Lieres, H. Offermann, R. Westphal, M. Pohl, D. Rother, *Angew. Chem. Int. Ed.* **2013**, *52*, 6772–6775; g) T. Sehl, H. C. Hailes, J. M. Ward, U. Menyes, M. Pohl, D. Rother, *Green Chem.* **2014**, *16*, 3341–3348; h) V. Erdmann, B. R. Lichman, J. Zhao, R. C. Simon, W. Kroutil, J. M. Ward, H. C. Hailes, D. Rother, *Angew. Chem. Int. Ed.* **2017**, *56*, 12503–12507.

[5] a) J. H. Schrittwieser, S. Velikogne, M. Hall, W. Kroutil, *Chem. Rev.* **2018**, *118*, 270–348; b) J. M. Sperl, V. Sieber, *ACS Catal.* **2018**, *8*, 2385–2396.

[6] C. Claaßen, T. Gerlach, D. Rother, *Adv. Synth. Catal.* **2019**.

[7] a) E. Danieli, J. Perlo, A. L. L. Duchateau, G. K. M. Verzijl, V. M. Litvinov, B. Blümich, F. Casanova, *ChemPhysChem* **2014**, *15*, 3060–3066; b) S. Kern, K. Meyer, S. Guhl, P. Gräßer, A. Paul, R. King, M. Maiwald, *Anal. Bioanal. Chem.* **2018**, *410*, 3349–3360; c) D. Cortés-Borda, E. Wimmer, B. Gouilleux, E. Barré, N. Oger, L. Goulamaly, L. Peault, B. Charrier, C. Truchet, P. Giraudeau, M. Rodriguez-Zubiri, E. Le Grognec, F.-X. Felpin, *J. Org. Chem.* **2018**, *83*, 14286–14299; d) B. Blümich, K. Singh, *Angew. Chem. Int. Ed.* **2018**, *57*, 6996–7010; e) M. V. Silva Elipe, R. R. Milburn, *Magn. Reson. Chem.* **2016**, *54*, 437–443.

[8] a) D. Kreyenschulte, E. Paciok, L. Regestein, B. Blümich, J. Büchs, *Biotechnol. Bioeng.* **2015**, *112*, 1810–1821; b) R. Legner, A. Wirtz, T. Koza, T. Tetzlaff, A. Nickisch-Hartfiel, M. Jaeger, *Biotechnol. Bioeng.* **2019**, *116*, 2874–2883.

[9] a) K. A. Farley, U. Reilly, D. P. Anderson, B. P. Boscoe, M. W. Bundesmann, D. A. Foley, M. S. Lall, C. Li, M. R. Reese, J. Yan, *Magn. Reson. Chem.* **2017**, *55*, 348–354; b) R. Legner, A. Wirtz, M. Jaeger, *J. Spectrosc.* **2018**, *2018*; c) L. Sparlinek, V. Leitner, B. Kamm, *J. Biotechnol.* **2018**, *284*, 63–67.

[10] a) M. V. Gomez, A. de la Hoz, *Beilstein J. Org. Chem.* **2017**, *13*, 285–300; b) D. Bouillaud, J. Farjon, O. Gonçalves, P. Giraudeau, *Magn. Reson. Chem.* **2019**, 1–11.

[11] D. Koszelewski, K. Tauber, K. Faber, W. Kroutil, *Trends Biotechnol.* **2010**, *28*, 324–332.

[12] a) D. Gocke, T. Graf, H. Brosi, I. Frindi-Wosch, L. Walter, M. Müller, M. Pohl, *J. Mol. Catal. B* **2009**, *61*, 30–35; b) J. Döbber, T. Gerlach, H. Offermann, D. Rother, M. Pohl, *Green Chem.* **2018**, *20*, 544–552.

[13] D. Rother, G. Kolter, T. Gerhards, C. L. Berthold, E. Gauchenova, M. Knoll, J. Pleiss, M. Müller, G. Schneider, M. Pohl, *ChemCatChem* **2011**, *3*, 1587–1596.

[14] R. L. Hanson, B. L. Davis, Y. Chen, S. L. Goldberg, W. L. Parker, T. P. Tully, M. A. Montana, R. N. Patel, *Adv. Synth. Catal.* **2008**, *350*, 1367–1375.

[15] Á. G. Baraibar, E. von Lieres, W. Wiechert, M. Pohl, D. Rother, *Top. Catal.* **2014**, *57*, 401–411.

[16] P. Tufvesson, J. Lima-Ramos, J. S. Jensen, N. Al-Haque, W. Neto, J. M. Woodley, *Biotechnol. Bioeng.* **2011**, *108*, 1479–1493.

[17] S. Sun, M. Jin, X. Zhou, J. Ni, X. Jin, H. Liu, Y. Wang, *Molecules* **2017**, *22*, 1517.

[18] D. Besghini, M. Mauri, R. Simonutti, *Appl. Sci. Res.* **2019**, *9*.

[19] a) M. Maiwald, H. H. Fischer, Y.-K. Kim, K. Albert, H. Hasse, *J. Magn. Reson.* **2004**, *166*, 135–146; b) U. Holzgrabe, *Prog. Nucl. Magn. Reson. Spectrosc.* **2010**, *57*, 229–240.

[20] D. L. Rabenstein, D. A. Keire, *Quantitative chemical analysis by nmr*, Marcel Dekker Inc, United States, **1991**.

[21] N. Bloembergen, E. M. Purcell, R. V. Pound, *Phys. Rev.* **1948**, *73*, 679–712.

[22] a) T. D. W. Claridge, *High-resolution nmr techniques in organic chemistry*, 2nd ed., Elsevier, Amsterdam, Boston, **2009**; b) W. S. Price, *Concepts Magn. Reson. Part A* **2009**, *34a*, 60–61; c) H. Friebolin, *Basic one- and two-dimensional nmr spectroscopy*, Wiley, **2005**.

[23] International conference on harmonisation of technical requirements for registration of pharmaceuticals for human use "*Validation of analytical procedures: Text and methodology q2(r1)*", **2005**, https://www.ich.org/fileadmin/Public_Web_Site/ICH_Products/Guidelines/Quality/Q2_R1/Step4/Q2_R1_Guideline.pdf.

[24] A. M. R. Hall, J. C. Chouler, A. Codina, P. T. Gierth, J. P. Lowe, U. Hintermair, *Catal. Sci. Technol.* **2016**, *6*, 8406–8417.

[25] a) J. S. Shin, B. G. Kim, *Biotechnol. Bioeng.* **1997**, *55*, 348–358; b) H.-S. Bea, Y.-M. Seo, M.-H. Cha, B.-G. Kim, H. Yun, *Biotechnol. Bioprocess Eng.* **2010**, *15*, 429–434; c) M. S. Malik, E.-S. Park, J.-S. Shin, *Green Chem.* **2012**, *14*, 2137–2140; d) W. Böhmer, T. Knaus, A. Volkov, T. K. Slot, N. R. Shiju, K. Engelmark Cassimjee, F. G. Mutti, *J. Biotechnol.* **2019**, *291*, 52–60.

[26] a) R. Oeggl, T. Maßmann, A. Jupke, D. Rother, *ACS Sustainable Chem. Eng.* **2018**, *6*, 11819–11826; b) J. Wachtmeister, A. Jakoblinnert, D. Rother, *Org. Process Res. Dev.* **2016**, *20*, 1744–1753.

Manuscript received: October 9, 2019
Revised manuscript received: November 19, 2019
Accepted manuscript online: December 5, 2019
Version of record online: January 20, 2020